CONVECTION HEAT TRANSFER COEFFICIENTS IN DE LAVAL NOZZLES

TECHNICAL REPORT NO. HS-3

NAVY CONTRACT N6-onr-251 TASK ORDER 6
(NR-090-104)

Department of Mechanical Engineering
Stanford University
Stanford, California

October 1, 1951

Prepared By:
R. K. Pefley

Approved by:
A. L. London
Project Supervisor

ABSTRACT

The objectives of this program are to determine the local convection heat transfer coefficients in the convergent portion and throat sections of de Laval nozzles; and to determine the effect on the local heat transfer coefficients, particularly at the throat, of varying the contour in the converging section of the nozzle.

Three two-dimensional nozzles ~~(described hereafter as III, IV, V), with pressure gradients as defined in Fig. 1a, and resulting cross-sectional areas as described in Fig. 1b,~~ have been tested. Heat transfer coefficients have been obtained for both the flat and contoured walls.

The results do not correlate when using a length dimension based on hydraulic diameter, as conventionally employed for established pipe flow.

The results, for both the flat and contoured walls, do correlate, when using a length dimension measured from the nozzle entrance along the walls. However, the heat transfer coefficients are higher than for turbulent boundary layer flat-plate flow. This appears to be partially due to the technique used in obtaining the apparently local coefficients, and partially due to the negative pressure gradient effect.

A significant result of these tests is that the throat coefficients, for the same mass flow rates through all the nozzles III, IV, and V, agree within ± 15%, indicating that the markedly different throat approach contour variations shown in Fig. 2 do not produce significant variations in the nozzle throat coefficients.

A theoretical solution, predicting the local heat transfer coefficients along the flat wall of nozzle III, has been made by introducing the pressure gradient of nozzle III into the von Kármán boundary layer momentum equation. The results of this work are compared to the experimental findings, and are utilized to interpret the experimental results.

TABLE OF CONTENTS

REFERENCES

(a) "Transient Heat Conduction in Hollow Cylinders after Sudden Change of Inner Surface Temperature", by R. L. Perry and W. P. Berggren, University of California Publications in Engineering, Vol. 5, No. 3, pp 59-88.

(b) "Convection Heat Transfer Coefficients in de Laval Nozzles", by S. J. Kline, T. R. No. HS-2, N6-ONR-251, T. O. 6, Stanford University, June 30, 1950.

(c) "Convection Heat Transfer Coefficients in Rocket Nozzles", by S. J. Kline, Preliminary Report, Stanford University Department of Mechanical Engineering, December 12, 1949.

(d) "Some Experiments on the Heat Transfer from a Gas Flowing Through a Convergent-Divergent Nozzle", by O. A. Saunders and P. H. Calder, a paper presented at the 1951 Heat Transfer and Fluid Mechanics Institute, Stanford University, California.

(e) "Study of Convective Heat Transfer Coefficients in a de Laval Nozzle", by B. Sze, an unpublished report, Stanford University, Department of Mechanical Engineering.

(f) "The Effect of an Arbitrary Surface Temperature Variation Along a Flat Plate on the Convective Heat Transfer in an Incompressible Fluid with Turbulent Boundary Layer", by M. W. Rubesin, NACA TN 2345, April, 1951.

(g) "Handbook of Supersonic Aerodynamics", Bureau of Ordnance, Vol. I and II, Oct. 1950.

(h) "Introduction to the Transfer of Heat and Mass", E. R. G. Eckert, 1st Edition, McGraw-Hill Book Co., 1950.

(i) "Heat Transfer", by M. Jakob, Vol. I, John Wiley and Sons, 1949.

(j) "Heat Transmission", by W. H. McAdams, Second Edition, McGraw-Hill Book Co., 1942.

(k) "An Investigation of Aircraft Heaters, by Tribus and Boelter, II Properties of Gases, NACA Wartime Report, ARR, October, 1943.

(l) "Heat Transfer, Local and Average Coefficients for Air Inside Tubes", by A. Cholette, Chemical Engineering Progress, Vol. 44, No. 1, pp. 81-88.

(m) "Heat Transfer in a Turbulent Liquid or Gas Stream", by H. Latzko, NACA Technical Memorandum No. 1068, October, 1944.

(n) "A Method of Correlating Forced Convection Heat Transfer Data and a Comparison with Fluid Friction", by A. P. Colburn, Transactions Am. Inst. Chem. Eng., Vol. 29, 1933, pp. 174-210.

(o) "Aerodynamic Heating and Convective Heat Transfer - Summary of Literature Survey", by H. A. Johnson and M. W. Rubesin, A. S. M. E. Transactions, Vol. 71, No. 5, July 1949.

(p) "Determination of Rocket Motor Heat Transfer Coefficients by the Transient Method", by S. Greenfield, paper xvi presented at Heat Transfer and Fluid Mechanics Institute, June 1950.

(q) "Heat Transfer Coefficients for Air Flowing in Round Tubes, in Rectangular Ducts, and Around Finned Cylinders", by R. E. Drexel and W. H. McAdams, N.A.C.A. Wartime Report, February, 1945.

NOMENCLATURE

English Letter Symbols

A - heat transfer area, ft^2

a - length, ft

C - specific heat of solid materials, Btu/(lb ^oF)

c_p - specific heat of fluid at constant pressure, Btu/(lb$_x$ ^oF)

D - hydraulic diameter of nozzles, $4\ r_h$, ft

G - mass flow velocity, lbs/(hr ft^2)

h - unit convective heat transfer coefficient, Btu/(hr ^oF ft^2)

k - thermal conductivity, Btu/(hr ft^2 ^oF/ft)

L - total nozzle length to throat, ft

m - arbitrary length dimension, ft

p - pressure, lbs/ft^2

q - heat flow rate, Btu/hr

r - radius from center of plug, ft

t - temperature, ^oF

V - total volume of copper plug, ft^3

x - distance from nozzle entrance measured along the wall profile, ft

Greek Letter Symbols

α - thermal diffusivity, ft^2/hr

δ - boundary layer thickness, ft

Δ - finite difference

ρ - density, lbs/ft^3

θ - time, hr

μ - viscosity lbs/(hr ft)

Dimensionless Groups

St - Stanton's Number $h/G\ c_p$

Pr - Prandtl's Number $\mu\ c_p/k$

Nu - Nusselt's Number $h\ x\ /k$ or hD/k

Re - Reynold's Number $G\ x/\mu$ or GD/μ

M - Mach Number

Subscripts

b - denotes bakelite matrix

aw - denotes adiabatic wall temperature

o - denotes stream stagnation conditions

θ - denotes thermal plug variable with respect to time

1 - denotes conditions between thermal plug and gas stream

2 - denotes conditions between thermal plug and bakelite matrix

T - denotes total

r - denotes any constant radius

INTRODUCTION

A detailed description of the purpose, proposed test program, test apparatus and some test results has been made in two previous reports, references (d) and (e). To facilitate reading this report these topics will be briefly summarized.

Objectives of Program

To determine the local convection heat transfer coefficients in the convergent section of a series of de Laval nozzles.

To discover whether or not modification of the curvature of the nozzle wall approaching the throat section will have significant influence on the convection coefficients at the throat.

To formulate correlations of results that may be useful to rocket designers and others concerned with heat transfer in nozzles.

Test Program

To test a series of five two dimensional nozzles, the only variables being the throat approach contour and the mass flow rate.

To make further tests and modifications to the test apparatus as dictated by the results obtained from these experiements.

Test Apparatus

The series of nozzles are made from bakelite to minimize the undesirable heat loss and yet have sufficient strength to prevent distortion or leakage. They are two dimensional; i.e., one pair of opposite walls is flat and one pair is curved.

Copper plugs, 3/8 inches in diameter, are buried in one flat wall of the nozzle and one curved wall, and are spaced uniformly along the axis of the nozzles. Their faces are machined flush with the faces of the bakelite (See Fig. 2).

Local heat transfer coefficients are obtained by a transient technique. The copper plugs are heated by a hot iron pressed against their back side -- then cooled by the high velocity gas stream sweeping their front side.

Previously Reported Results

Local heat transfer coefficients were reported for the contour walls of nozzles II and III. Sufficient data was not available to permit correlation in any suitable form.

The limited results tentatively indicated that a considerable variation in the local heat transfer coefficient at the throat might be experienced by modifying the throat approach contour.

Purpose of Current Report

(a) To analyze results obtained in terms of available theory and conventional correlations.

(b) To further consider, in the light of additional data, the tentative conclusion that contour variation in the convergent section would have a considerable effect on the throat heat transfer coefficient.

(c) To describe a theoretical attempt to predict the local coefficients in a nozzle, neglecting the effect of wall curvature but considering the effect of pressure gradient.

SUMMARY OF RESULTS AND CONCLUSIONS

For this method of testing and with the nozzle contour variations described in the body of the report, the variation in throat coefficient as a function of modification of wall curvature is not great enough to single out any one contour as being preferred. The variation in contour produces considerable local variation in coefficient due to wall curvature, but this effect, along with the effect of pressure gradient variation, does not persist into the throat section.

The data obtained clearly demonstrates that prediction of heat transfer coefficients in the convergent portion of a de Laval nozzle should be made on a flat plate or pipe entrance type of correlation, (Contrast Figs. 4a, b and 5a, b).

If the nozzle is long (L/D large based on throat hydraulic diameter) it is possible to predict a throat coefficient based on the correlation (from reference (q))

$$Nu \; Pr^{-1/3} = .021 \; Re_D^{.8}$$

which will be higher than predicted on the flat plate correlation (from reference (n))

$$Nu \; Pr^{-1/3} = .0295 \; Re_x^{.8}$$

For this case, experimental evidence indicates the pipe flow correlation would be the preferred basis for predicting the coefficients in the throat section. This is not to be construed as indicating that the velocity profile in the throat section of the nozzle would be the same as for established pipe flow. Reference (p) reports correlation of data for rocket combustion chambers and nozzles on this basis. It may be seen in Figs. 5a, b that the local coefficients obtained for the throat section in the experiment are of magnitudes corresponding to the established pipe flow behavior.

The method of testing, using small thermal plugs to obtain the local heat transfer coefficients, results in a delayed thermal boundary layer with respect to the origination of the hydrodynamic boundary layer. This condition would not exist in a nozzle with heat transfer throughout. Reference (f) gives a theoretically predicted correction for this effect in the case of turbulent

boundary layer flow over a flat plate. When this correction is introduced, the experimental results agree surprisingly well with the flat plate equation

$$Nu\ Pr^{-1/3} = .0295\ Re_x^{.8}$$

The difference between Figs. 4a and 4b, 5a and 5b is the introduction of this compensating factor.

The good agreement with flat plate data may be in part fortuitous since the correction described above is predicted for flat plate flow with no longitudinal pressure gradient; whereas, the nozzle flow is subjected to severe axial pressure gradients.

A boundary layer analysis, utilizing 99% of the free stream velocity as the thickness of the boundary layer; the boundary layer momentum equation of von Kármán and the pressure gradient of nozzle III, has been made, reference (e). The results indicate that the influence of nozzle III pressure gradient on the flat wall hydrodynamic boundary layer will reduce the boundary layer thickness in the throat section by 70% when compared to the flat plate hydrodynamic boundary layer with no pressure gradient. This results in an estimate that the heat transfer coefficient at the throat should be approximately 30% higher than predicted by the flat plate correlation.

From these arguments, it is possible that the use of the thermal plugs tends to conceal the effect of the pressure gradient by departing from the correction as evaluated from reference (f). This remains to be demonstrated.

Until more experimental evidence is obtained it is recommended that the flat plate correlation

$$Nu\ Pr^{-1/3} = .0295\ Re_x^{.8}$$

be used to predict the local heat transfer coefficients in the convergent portion of a de Laval nozzle.

For the divergent portion of the de Laval nozzle, reference (d) reports correlation of results for a particular nozzle by the equation

$$St = .0285\ Re_x^{-.2}$$

The length in the Reynolds Number is measured from the throat of the nozzle.

It is worthwhile to compare the results of reference (d) with the results of this experiment since the two sets of data overlap at the throat section of the nozzles. This has been done using the local hydraulic diameter as the characteristic length. The data are in fair agreement as can be seen in Fig. 6. Some correction of data of reference (d) is in order for there appears to be a delayed thermal boundary layer in this test apparatus also. This correction would bring the two sets of data into better agreement.

EXPERIMENTAL METHODS

Modification of Experimental Apparatus

Results reported previously were for copper plugs buried in the curved wall only. For the tests reported here of nozzles III, IV, and V, plugs have been buried along the centerline of the flat wall of the nozzles as well.

Modification of Method of Reducing Data

The procedure used in reducing the data reported in HS-2, reference (b), was inadequate. The source of error resulted from the heat loss from the copper plug to the bakelite surrounding it being approximated by the equation:

$$q_2 = h_2 A_2 (t_\theta - t_{aw})$$

where h_2 was evaluated by taking runs with no flow through the nozzle. This value was then subtracted from the coefficient obtained by reducing the transient data, for flow in the nozzle, in the standard fashion.

Actually the heat loss to the bakelite is represented by the equation:

$$q_2 = k_b A_2 \left(\frac{\partial t}{\partial r}\right)_b$$

where k_b, $\left(\frac{\partial t}{\partial r}\right)_b$ are conditions of the bakelite at the copper plug-bakelite interface, and for the actual conditions $\left(\frac{\partial t}{\partial r}\right)_b$ is a variable throughout the test run.

It was determined by a graphical solution that for the conditions of the tests and with the materials used, $\left(\frac{\partial t}{\partial r}\right)_b$ reverses sign during the cooling run in the usable portion of the time-temperature cooling curve. At the time $\left(\frac{\partial t}{\partial r}\right)_b = 0$ there is no heat loss to the bakelite and the slope of the time-log temperature curve in this region will be $\frac{h_1 A_1}{V \rho C}$, from which h_1 can be evaluated.

Use was made of this fact to reduce the data for this report. The heat transfer coefficient was obtained by drawing a straight line through the points on the time-temperature cooling curve in the region where $(\frac{\partial t}{\partial r})_b$ was predicted to be near zero. The predicted location of $(\frac{\partial t}{\partial r})_b = 0$ was justified initially by observing that the time-temperature curve became straight in this region, which it should for no heat leakage. An example time-temperature curve from which the slope has been defined is shown in Fig. (8).

Because heating time is important in predicting the point, $(\frac{\partial t}{\partial r})_b = 0$, and since it was not held constant in previous test work, the data available was not recalculated. Instead, nozzle III has been retested. Nozzle II was not retested since it was decided that nozzles III, IV, and V would give adequately descriptive results. The results of testing nozzles III, IV, and V are reported here.

EXPERIMENTAL RESULTS

The data of principal interest are the local heat transfer coefficients at the throat of the nozzles and the influence of the various wall curvatures on these coefficients. Fig. 3 best describes these results. From this figure it may be observed that for the high mass flows ($G = 5.2 \times 10^5$ at the throat), the local coefficients for all nozzles for both the contour and flat walls just after the throat section, may be described by $h_1 = 350 \pm 10\%$. Note however, that the curved wall coefficients vary over a considerable range, $h_1 = 310$ to 380. The flat wall coefficients vary only from $h_1 = 360$ to 385 which is within the range of the experimental accuracy of the test apparatus.

The flat wall of the nozzles is relatively free of wall curvature effects, and hence these results indicate that the variation of negative pressure gradients of the magnitude found in the test nozzles has only minor influence on the local heat transfer coefficients at the throat.

The effect of wall curvature is more significant. Since there is no difference in wall curvature in the three nozzles precisely at the throat or thereafter, the variation in the local coefficient (310 to 380) among the three nozzles is assumed to be the relative effect of different curvatures upstream in the nozzles that has persisted to the throat.

Greater evidence of the influence of wall curvature can be observed by examining the curved wall coefficients of the nozzles upstream of the nozzle throats. Here it is seen that the wall curvature has a marked effect on the local coefficient. A concave curvature such as in nozzle IV produces a coefficient 40% lower than that realized by the flat wall in the same location along the nozzle axis. The converse is true for the sharp convex curvature found in nozzle V, where the curved wall coefficient is about 40% higher than that realized by the flat wall in the same location.

Figs. 4a, b, and 5a, b demonstrate that the heat transfer behavior in the convergent portion of the nozzles more nearly approximates flat plate rather than pipe flow behavior. The results in Figs. 4a and 5a are high. This is due to the fact that for the experimental tests small thermal plugs were used which results in a delayed thermal boundary layer with respect to the initiation of the hydrodynamic boundary layer. This effect has been taken into account in plotting the data in Figs. 4b and 5b. The results in

Fig. 4b show good agreement with the flat plate correlation for heat transfer

$$Nu\ Pr^{-1/3} = .0295\ Re_x^{.8}$$

Fig. 5b demonstrates that prediction of heat transfer coefficients in the convergent portion of a nozzle using the conventional established pipe flow correlation would lead to results considerably below the actual conditions. However, it is to be noted that at the throat section the coefficients agree with established pipe-flow coefficients.

The experimental results obtained for the throat section of the nozzles have been compared to those reported in reference (d) for the throat and divergent portion of a particular nozzle. This comparison is shown in Fig. 6 using the local hydraulic diameter as the characteristic length in evaluating the Reynolds Number. The experimental data of this report have been modified by the correction factor for the delayed thermal boundary layer, as described earlier. The data of reference (d) have been altered by the author, in that the viscosity has been evaluated on an estimated average value between the wall temperature and the stream temperature. The original data was reported using the viscosity based on the stream stagnation temperature. These data are in fair agreement.

The test apparatus used in reference (d) appears to introduce a delayed thermal boundary layer. Compensation for this effect would bring the data into better agreement.

In Fig. 7 the heat transfer coefficients for the plugs located on either side of the throat section are plotted using the conventional flat plate dimensionless groups and introducing the correction factor just described.

Fig. 10a compares, for a particular mass flow, the experimental local heat transfer coefficients obtained along the flat wall of nozzle III to:

a) The local heat transfer coefficient predicted by the flat plate correlation

$$Nu_x Pr^{-1/3} = .0295\ Re_x^{.8}$$

b) The local heat transfer coefficient as predicted from reference (m) for unestablished flow in pipes.

c) The local heat transfer coefficient predicted from the boundary layer thickness as influenced by the pressure gradient of nozzle III.

d) The experimental local heat transfer coefficient corrected as suggested in reference (f) for the delayed thermal boundary layer effect.

Figs. 10b and c compare the local predicted flat plate coefficients, the experimental flat wall coefficients, and the experimental local coefficients taking into account the delayed thermal boundary layer effect. These comparisons are for the flat walls of nozzles IV and V respectively, and the same mass flows ($G = 5.2 \times 10^5$ at the throat). It is seen that in all cases, in the throat region, the corrected predicted results agree surprisingly well with the experimental results.

Figure 1a	Pressure ratio versus distance from nozzle entrance for test nozzle contours III, IV, V.
Figure 1b	Nozzle area versus distance from nozzle entrance for test nozzle contours III, IV, V.
Figure 2a	Picture of bakelite contour with embedded copper plugs and brass counterpart, nozzle IV.
Figure 2b	Picture of nozzle IV with one flat wall removed. Note copper plugs buried in flat wall.

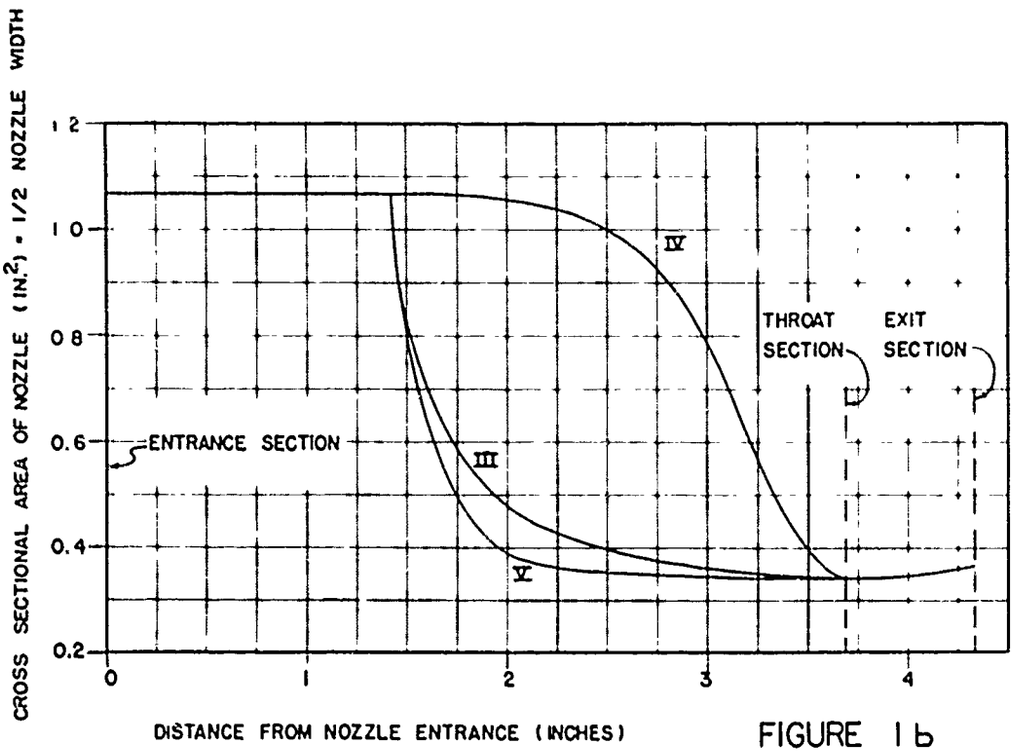

FIGURE 1b

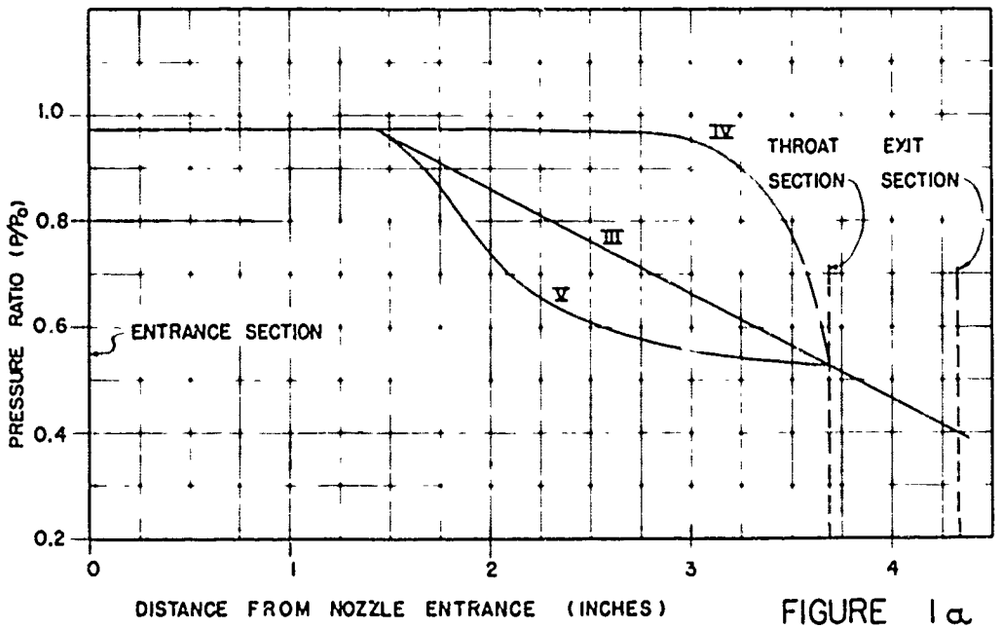

FIGURE 1a

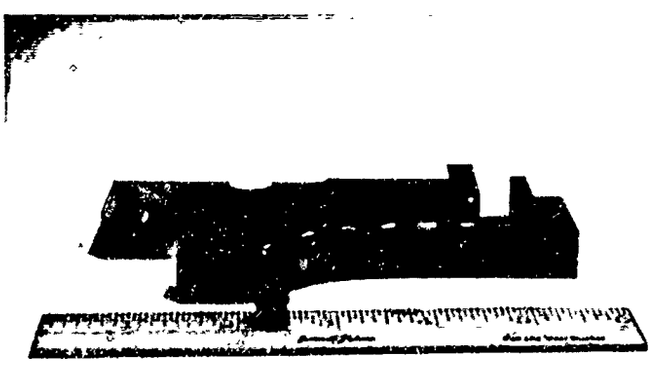

FIG. 2a

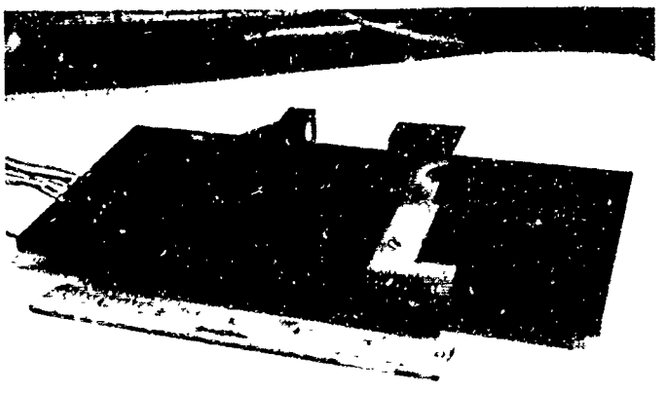

FIG 2b

Figure 3 Local apparent heat transfer coefficients versus distance from nozzle entrance for test nozzles III, IV, V.

⊙ Points are coefficients obtained from contoured walls of nozzles.

⊡ Points are coefficients obtained from flat walls of nozzles.

——— — ——— Curves are for high mass flow. $G = 5.2 \times 10^5$ at nozzle throats and M = 1 .

———— Curves are for low mass flow.
$G = 3.5 \times 10^5$ at nozzle throats for nozzles IV and V and M = 1.
$G = 2.6 \times 10^5$ and M = .85 at nozzle throat for nozzle III.

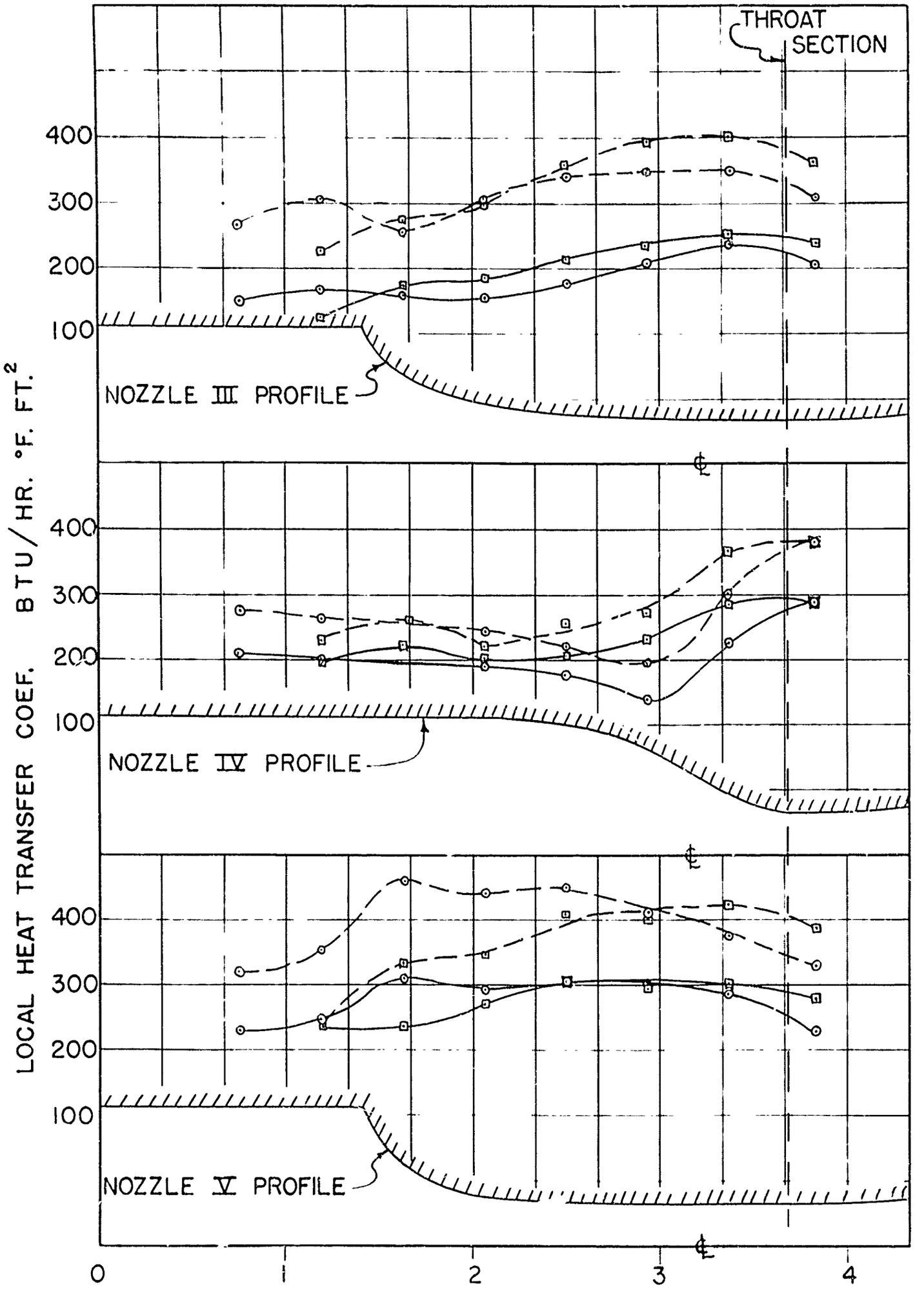
THROAT SECTION
400
300
200
100
NOZZLE III PROFILE
NOZZLE IV PROFILE
NOZZLE V PROFILE
LOCAL HEAT TRANSFER COEF. BTU/HR. °F. FT.²
0
1
2
3
4
DISTANCE FROM NOZZLE ENTRANCE INCHES

FIGURE 3

Figure 4a — Experimental data for nozzles III, IV, V are plotted in dimensionless form, using distance measured from the nozzle entrance along nozzle profile as characteristic length dimension.

$Nu\ Pr^{-1/3}$ Versus Re_x

Figure 4b — Same as Figure 4a except that compensating factor for delayed thermal boundary layer (from reference f) has been used to correct data for this effect.

Figure 5a — Experimental data for nozzles III, IV, V are plotted in dimensionless form using local hydraulic diameter as the characteristic length dimension.

$Nu\ Pr^{-1/3}$ Versus Re_D

Figure 5b — Same as Figure 5a except that the compensating factor for delayed thermal boundary layer (from reference f) has been used to correct data for this effect.

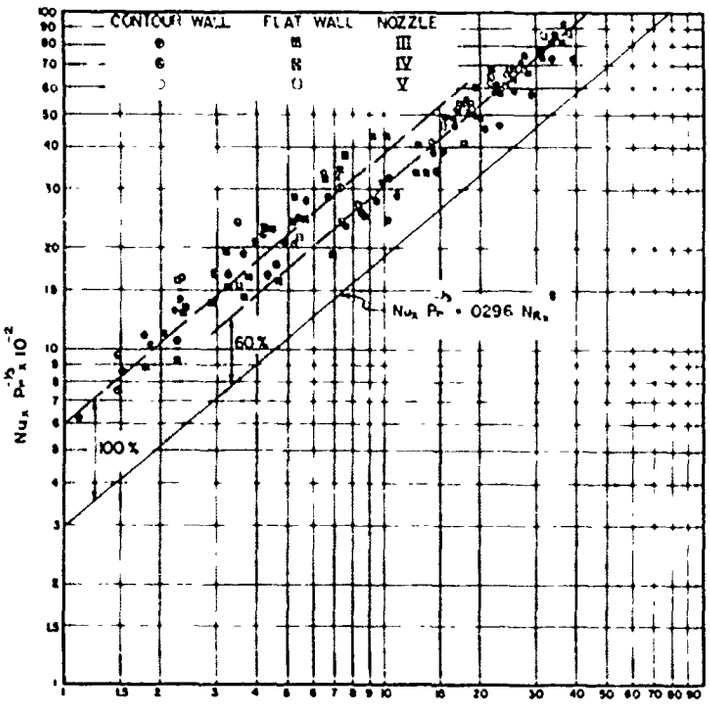

FIGURE 4a

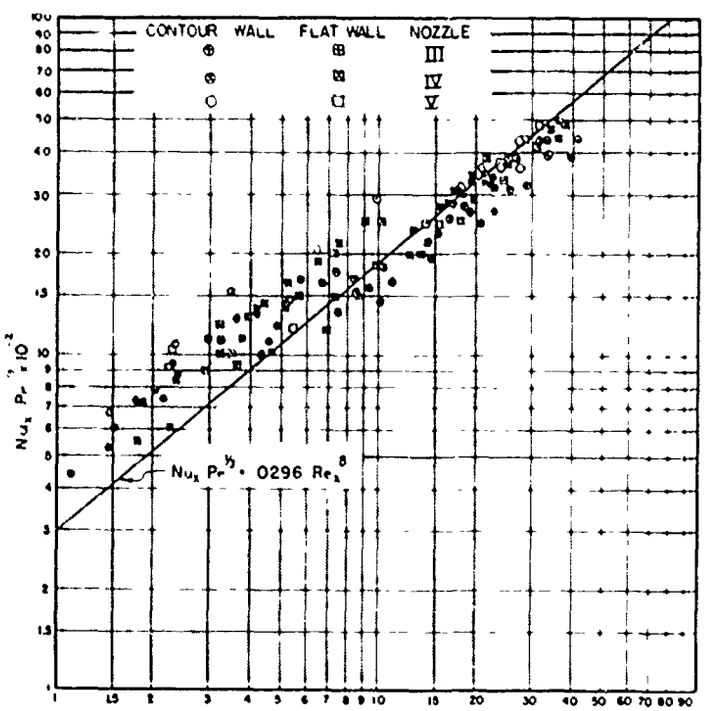

FIGURE 4b

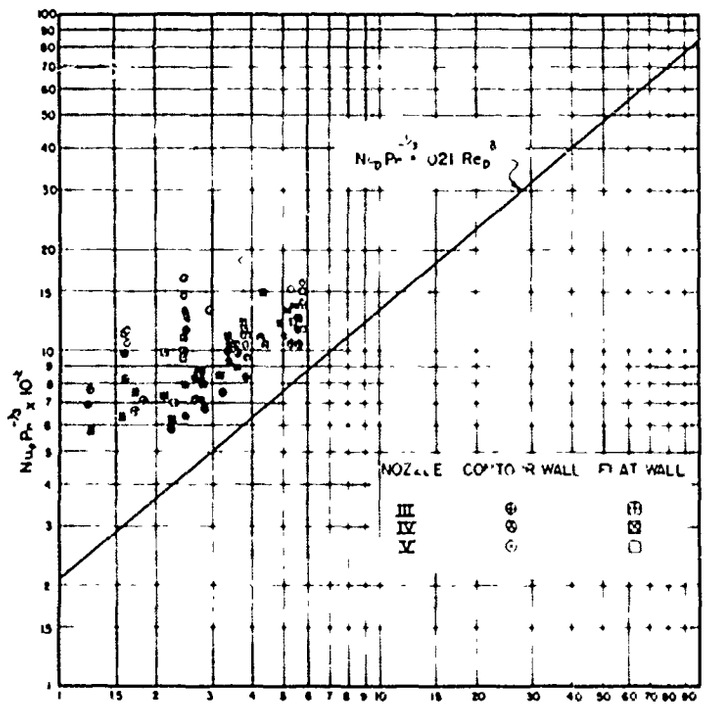

FIGURE 5a

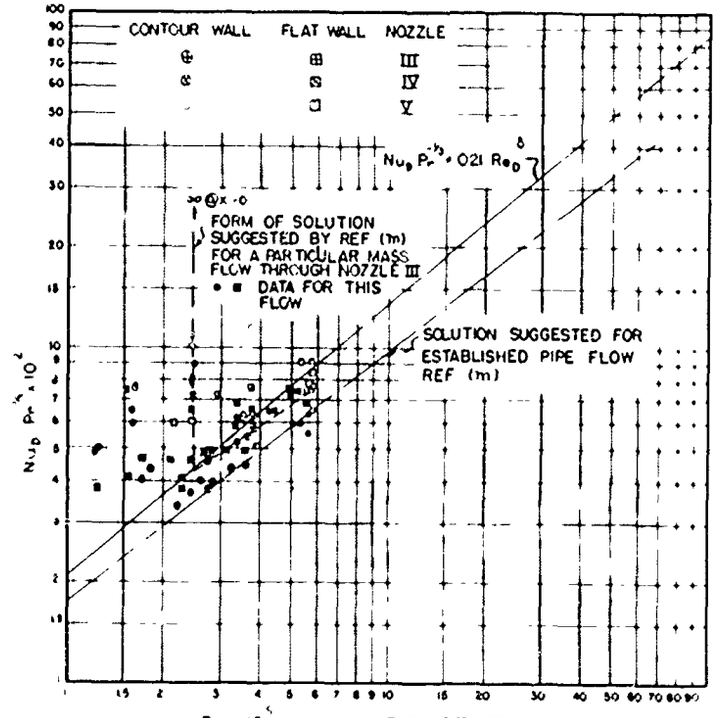

FIGURE 5b

Figure 6 Data for the throat sections of test nozzles III, IV, V, are plotted in dimensionless form after using the compensating factor for the delayed thermal boundary layer, reference (f). Also the data from reference (d) for the throat section and divergent section of a nozzle are plotted on the same dimensionless basis. Sections 1, 2, 3, 4, of reference (d) refer to the throat section and the subsequent three sections comprising the divergent portion of the nozzle respectively.

Figure 7 Data for two plugs nearest throat section on both contour and flat walls of nozzles III, IV, V are plotted on dimensionless basis using profile length from nozzle entrance as characteristic length. The data have been compensated for the delayed thermal boundary layer effect.

Figure 8 Sample Temperature-Time cooling curve of copper plug from which the heat transfer coefficient is deduced.

$\log(t_p - t_{aw})$ versus cooling time.

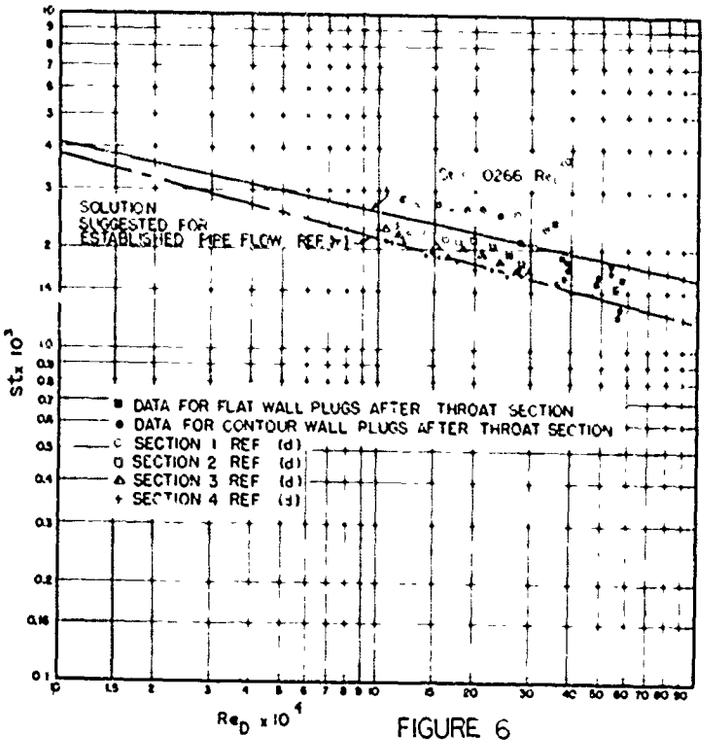

FIGURE 6

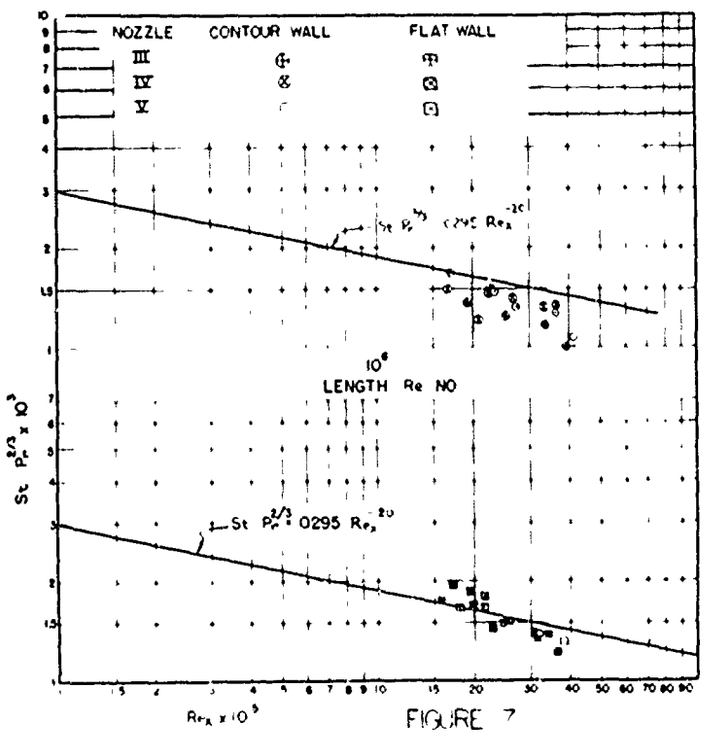

FIGURE 7

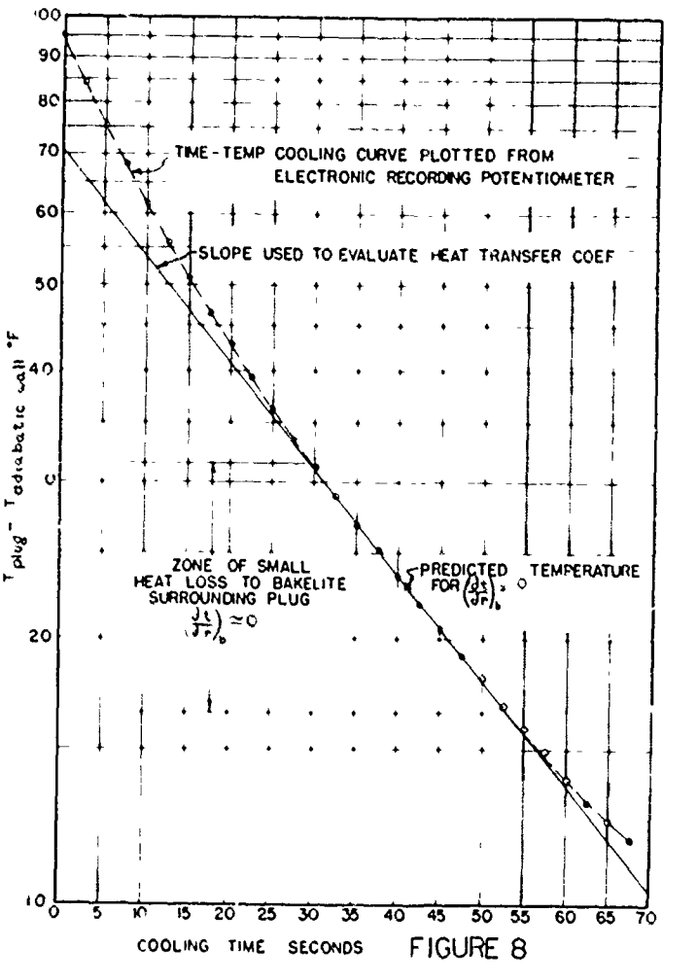

FIGURE 8

Figure 9. Curves are for a particular mass flow through nozzle III and are plotted versus distance from nozzle entrance.

(A) Flat plate turbulent boundary layer thickness.

(B) Flat plate boundary layer thickness as influenced by pressure gradient of nozzle III, reference (e).

(C) Mass flow velocity.

Figure 10a.

Curves, for a particular mass flow through nozzle III, pertain to flat wall of the nozzle and are plotted versus distance from nozzle entrance.

(D) Experimental local heat transfer coefficients.

(E) Predicted local coefficients on flat plate basis after introducing the pressure gradient of nozzle III, reference (e).

(F) Predicted local coefficients from flat plate correlation.

(G) Local coefficients predicted for unestablished flow in pipes, reference (m).

• Points are experimental coefficients corrected for delayed thermal boundary layer effect, reference (f).

Figures 10b, c.

Flat wall heat transfer coefficients are plotted versus distance from nozzle entrance for nozzles IV, V, respectively, and for

$$G = 5.2 \times 10^5$$

at nozzle throats.

⊙ Points are experimental data.

• Points are experimental data corrected for influence of delayed thermal boundary layer.

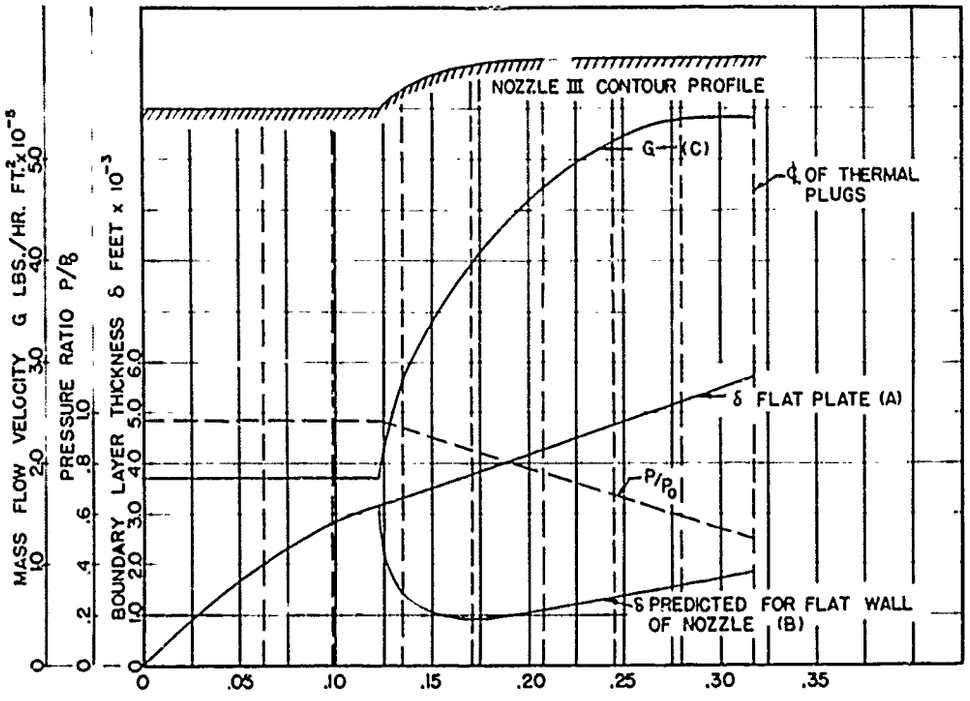

FIGURE 9

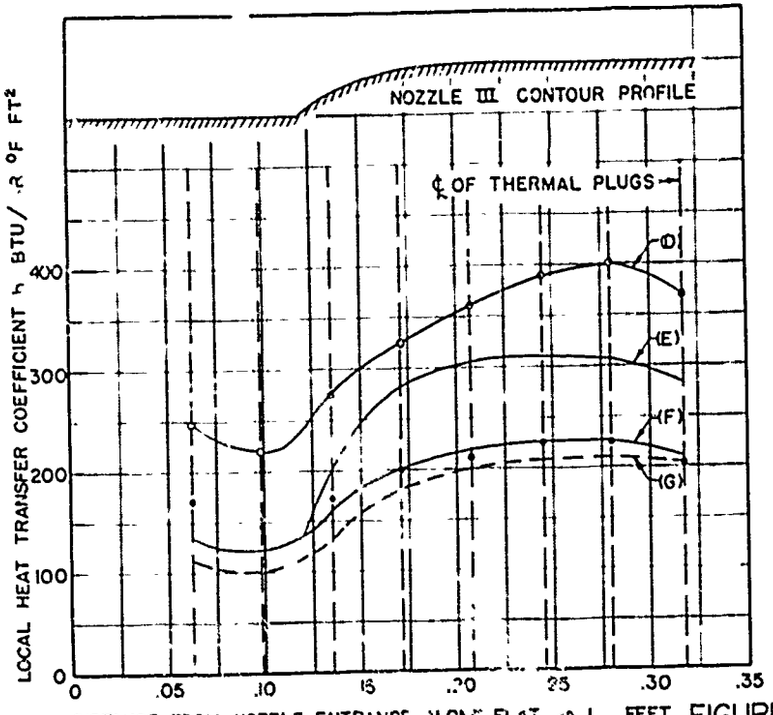

FIGURE 10a

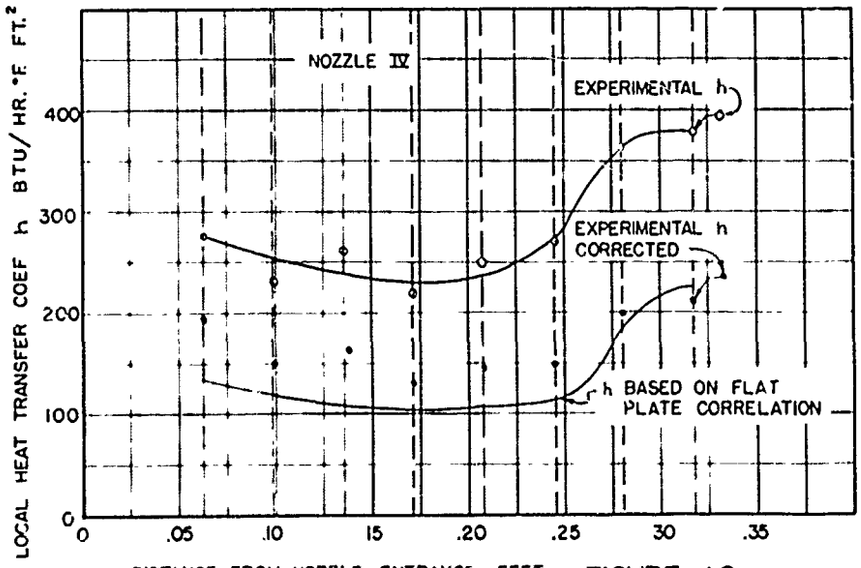

FIGURE 10 b

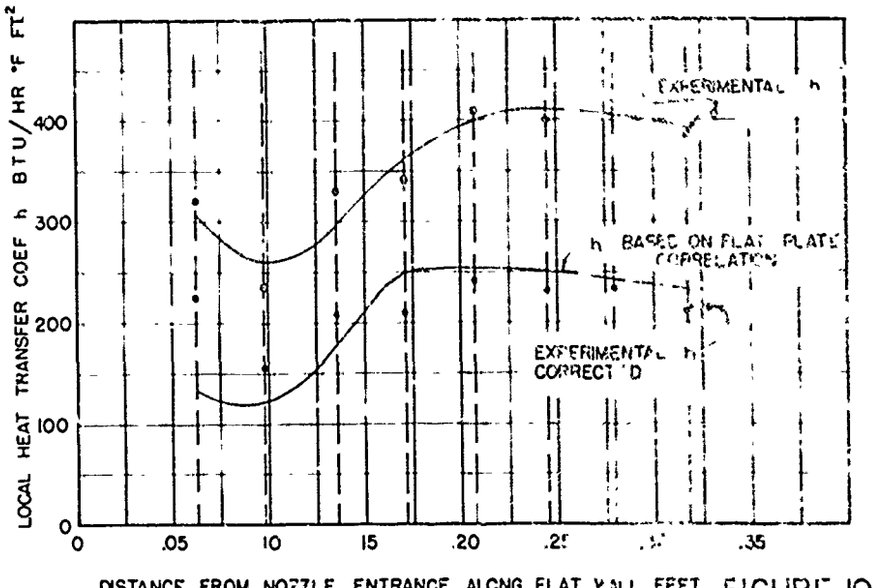

FIGURE 10c

DISCUSSION

Before discussing the results as they would apply to a conventional nozzle where heat transfer takes place continuously along the nozzle wall, it is necessary to give some consideration to the condition that in these tests the hydrodynamic and thermal boundary layers did not originate simultaneously. The hydrodynamic boundary layer starts at the entrance to the nozzle whereas the thermal boundary layer starts at the upstream edge of the heated plug. Neglecting for the moment the effects of pressure gradient, mass acceleration, and wall curvature; it is apparent that due to the delayed thermal boundary layer the heat transfer coefficients obtained by this experimental apparatus will be higher than would be expected in the duplicate nozzle with heat transfer throughout. Then the problem arises, to estimate quantitatively the effect of the delayed thermal boundary layer on the local heat transfer coefficient.

However, before this problem can be resolved, it is necessary to have some basis for predicting the local heat transfer coefficient for heat transfer throughout the nozzle. Two bases of prediction are possible. One, that the nozzle is so short, L/D of approximately 10 based on the throat hydraulic diameter, that the flow is unestablished and hence is essentially the same as flow over a flat plate. The other, that the flow is nearly established and hence the pipe flow correlation is a better basis of analysis.

That the flat plate basis is a superior starting point is apparent by examining Figs. 4a, b, and 5a, b. The data shows marked evidence toward correlation using distance from the nozzle entrance as the characteristic length whereas there is no correlation when using the local hydraulic diameter as the characteristic length.

Then the flat plate correlation suggested by Colburn, reference (n),

$$St\ Pr^{2/3} = .0295\ Re_x^{-.2}$$

will be utilized in the effort to estimate the influence of the delayed thermal boundary layer on the local heat transfer coefficient.

The basis of analysis could also be the pipe entrance flow behavior as predicted by reference (m). However, this equation is considerably more cumbersome to work with and gives results that agree quite well with the flat plate predictions (see Fig. 10a). Therefore, the flat plate correlation will be used.

Examination of Fig. 4 reveals that the experimental results are higher by 100% for the plugs near the nozzle entrance and about 60% higher for the plugs near the throat section when compared to the flat plate correlation.

The plugs near the nozzle entrance are not influenced by pressure gradient or wall curvature. Also, they are near the initiation of the hydrodynamic boundary layer so the flat plate flow behavior should be valid. Then the remaining factors causing these data to be 100% high are the delayed thermal boundary layer and abnormal nozzle entrance conditions. The nozzle entrance from the static chamber was made with large radius contours. Furthermore, these contours were varied and produced no significant change in the experimental results. Therefore, it is indicated that the delayed thermal boundary layer is the principal cause for the high data.

Consider the two possible extreme combinations of thermal and hydrodynamic boundary layer origination with respect to the thermal plug. The extreme which would give the lowest heat transfer coefficient for the plug would be if both thermal and hydrodynamic boundary layers originated at the nozzle entrance. The alternate extreme or one yielding the highest local heat transfer coefficient would be if both the thermal and hydrodynamic boundary layers originated at the leading edge of the plug.

Based on flat plate behavior, for all stream properties constant and free stream velocities identical, the local heat transfer coefficient h_1 is proportional to $x^{-.2}$ for turbulent boundary layer.

For the plugs near the nozzle entrance this gives a variation of h_1, based on the two extremes just described, of approximately 1.7, the latter coefficients being 70% higher. Then, if the actual plug behavior were near the upper limit of the two extremes it is expected that the data would be approximately 70% higher than the Colburn correlation predicts. That the results for the first plugs are on an average 30% higher than this upper limit cannot at this time be accounted for.

That the coefficients obtained experimentally should be nearer the upper limit than the lower limit can be justified. The more significant of the two boundary layer thicknesses with respect to heat transfer is the thermal boundary layer. Of the two extremes considered, the one with the thermal boundary layer starting at the leading edge of the thermal plug is much nearer the actual test conditions.

This argument was further substantiated by placing a thermal plug, identical with the test plugs, in the wall of a circular pipe. Here the flow was established turbulent flow. The two extremes between which the plug coefficient should lie in this case were; for the lower limit, the heat transfer coefficient predicted from the turbulent pipe flow correlation and for the upper limit, the coefficient assuming both the thermal and hydrodynamic boundary layers started at the leading edge of the plug. From the previous argument the results should be near the upper extreme value. This is the case. The upper value was predicted as 250% higher than the lower limit and the experimental values were 230% higher than this lower limit. These results agree with theory. Reference (m) predicts that the data should be 230% above the lower limit due to the effect of unestablished thermal boundary layer.

From this analysis it is concluded that the maximum delayed thermal boundary layer effect on the experimental values for the plugs near the nozzles' entrance would be to raise them approximately 60-70% higher than predicted by flat plate data.

In reference (f) a theoretical prediction is made of the effect of the delayed thermal boundary layer (wall temperature discontinuity) for turbulent flow over a flat plate. The results predicted for the plugs near the nozzle entrance, based on this reference, should be 40-60% higher than those for the case of heat transfer throughout the nozzle. For the plugs near the throat of the nozzle this reference predicts that the results will be 60-80% higher than for the case with heat transfer throughout. These values are in agreement with the foregoing analysis and have been used to eliminate the effect of the delayed thermal boundary layer in comparing the data to correlations where the thermal and hydrodynamic boundary layers originate simultaneously.

The plugs farther removed from the nozzle entrance are under the influence of pressure gradient, mass acceleration and wall curvature. That they show a strong tendency to correlate is indicative that these variables do not exert extreme influences with respect to the local heat transfer coefficients.

The delayed thermal boundary layer, based on the foregoing discussion, should cause these results also to be high by an approximate factor of 60-80%. This correction agrees with the experimental values. However, it is known that the negative pressure gradient has some influence on reducing the hydrodynamic boundary layer thickness and hence should raise the local heat transfer coefficient.

The effect of the negative pressure gradient has been quantitatively approximated for nozzle III for a particular mass flow. The von Karman boundary layer momentum equation, the 1/7th power velocity distribution, and the pressure gradient of nozzle III were utilized and integrated graphically to predict the boundary layer thickness as a function of distance from the nozzle entrance, reference (e). The results are shown in Fig. 9 compared to the boundary layer thickness based on flat plate flow, turbulent boundary layer and no pressure gradient. It is to be seen that the pressure gradient influence reduces the boundary layer thickness at the throat of the nozzle to approximately 1/4 of the value for no pressure gradient.

Using the boundary layer thickness predicted by this analysis, the local heat transfer coefficient was evaluated by the relation derived by Prandtl, which predicts h_1 as a function of fluid properties, wall shear stress, maximum velocity in the laminar sublayer, and free stream velocity.

The results are compared in Fig. 10 to the results predicted by the flat plate correlation and the results obtained by experiment for the flat side of nozzle III. It is seen that the predicted coefficient, considering pressure gradient, is approximately 30% higher in the throat region than the coefficient based on flat plate basis alone

Now if the delayed thermal boundary layer factor remained as predicted before consideration of pressure gradient and the pressure gradient influenced the coefficient as just described, the experimental coefficients for the plugs near the throat should be approximately 100% higher than predicted on the flat plate basis only. However, the delayed thermal boundary layer effect, since it is a function of the thermal and hydrodynamic boundary layers, will also be influenced by the negative pressure gradient. It should be reduced as a result of the reduction in thickness of the hydrodynamic boundary layer thickness. An estimate of this change, based on the graphically predicted boundary layer thickness, is that the experimental results should be 20-30% higher than for a continuously heated plate. Combining the two influences, the delayed thermal boundary layer and the pressure gradient, indicates that the results for the plugs near the

throat section should be 50-60% higher than predicted by the flat plate correlation. This is in agreement with the results obtained experimentally.

It is to be observed from the preceding discussion that it is possible for the delayed thermal boundary layer factor to conceal the effect of the negative pressure gradient by decreasing from the predicted value in amount equal to the increase in the local coefficient due to the pressure gradient effect. Whether or not this is so remains to be proven.

At this time, available theory does not permit the prediction of the local heat transfer coefficient under the influence of both pressure gradient and wall curvature. From the experimental results, see Fig. 3, it may be seen that in no case did the wall curvature produce a departure between the flat and contoured walls of more than 40%. Also when the results from the two walls are plotted in dimensionless form as in Figs. 4a, b and 5a, b, it is to be seen that they plot in the same manner although the scatter of the results for the contoured walls is greater.

It was anticipated initially that the results for the nozzles, particularly near the entrance, would be laminar, since the length Reynolds No. was less than 5×10^5. In no case were laminar heat transfer coefficients obtained. This is attributable to three possible causes. One, that the boundary layer is being heated and hence tends toward early transition; two, that even though the plugs are machined flush with the bakelite, the joint between the bakelite and the copper plug is not hydrodynamically clean and hence tends to promote turbulence in the boundary layer; three, that the stream entering the nozzle has sufficient degree of turbulence to promote early transition.

The topic of established versus non-established flow in the convergent portion of the de Laval nozzles should be discussed. Taking into account the correction factors discussed previously it is to be observed in Fig. 5 that the data in the throat region are in agreement with the coefficients predicted for established flow in pipes. It has been experimentally determined, references (l) and (m), that at an L/D of approximately 10 for the test flow conditions, the heat transfer coefficient is within 10% of that predicted for established pipe flow. If the nozzle throat hydraulic diameter is used, the maximum L/D is approximately 10. Therefore, the indication that the coefficients at the throat are approaching established pipe flow coefficients is to be expected. Therefore, if throat coefficients are of interest to a nozzle designer, the L/D value of the throat should be a design parameter.

Reference (d) has reported results for the throat and divergent sections of a particular de Laval nozzle. Based on the author's interpretation of an appropriate Reynolds number (using

$\frac{t_{stream} - t_{wall}}{2}$ to evaluate viscosity)

these results are shown in Fig. 6. Section 1 data of reference (d) are average coefficients in the nozzle throat section and hence can be compared with the throat section data reported here. It is to be seen that these data are in fair agreement.

In summary, it is anticipated that the local heat transfer coefficients in the convergent portion of the nozzle will agree essentially with flat plate coefficients. However, due to curvature and pressure gradient effects they may vary $\pm$ 30% from this value as the nozzle throat is approached. In the throat region they may be 30-40% high as a result of the negative pressure gradient although this is not proven. Furthermore, it is recommended that if calculation on a pipe Reynolds Number basis gives a higher coefficient than the flat plate Reynolds Number basis, it should be used for predicting the throat heat transfer coefficient, as a "conservative" design procedure.

The proposed future work on this project becomes apparent from the discussion of results obtained thus far:

a) Discover why the nozzle entrance coefficients are higher by 30% than can be justified.

b) Isolate the influence of pressure gradient on the delayed thermal boundary layer so that the data reported can be unquestionably used for the conditions of continuous heat transfer in the nozzle.

APPENDIX

METHOD OF DETERMINING THE HEAT TRANSFER COEFFICIENT FROM THE TIME-TEMPERATURE HISTORY OF THE THERMAL PLUG

The method of predicting the heat transfer coefficient to the gas stream using the thermal plug and transient technique would be a straight forward matter, if during the heating and the cooling of the plug, the heat loss to the bakelite matrix holding the plug were negligible.

For this transient case during cooling the heat transfer coefficient can be evaluated from the equation.

$$h_1 = \frac{V\rho C}{A_1} \frac{\log_e\left(\frac{t_\theta' - t_{aw}}{t_{\theta''} - t_{aw}}\right)}{\theta'' - \theta'} \qquad (1)$$

By plotting $(t_\theta - t_{aw})$ versus θ on semilog paper and using the slope of this plot the heat transfer coefficient h_1 can be evaluated directly.

This is not the case in the experimental apparatus under the conditions of test. During the cooling of the plugs the energy absorbed by the bakelite amounts to approximately 20% of the total thermal energy stored in the plugs during the heating process.

The value of 20% was predicted by a graphical solution of the time-temperature history in the bakelite. The graphical technique used, is presented in reference (a) and is a modification for radial heat flow of the Schmidt method.

Furthermore, if the heat loss from the plug to the phenolic were a constant with respect to time or varied with respect to $(t_\theta - t_{aw})$ some modification of equation (1) might be usable. But again, this is not the case. Therefore some other technique is necessary to evaluate the heat transfer coefficient to the gas stream.

In the experimental apparatus, neglecting heat transfer from the back side of the plugs which was found to be in all cases less than 3% of the heat transfer rate to the gas stream, heat flows from the plug via two paths. One into the high velocity gas stream, represented by the equation:

$$q_1 = h_1 A_1 (t_\theta - t_{aw}) \qquad (2)$$

The other is into the bakelite matrix surrounding the plug, represented by the equation:

$$q_2 = k_b A_2 \left(\frac{\partial t}{\partial r}\right)_b$$

Where $\left(\frac{\partial t}{\partial r}\right)_b$ is the radial temperature gradient in the bakelite at the contact face between the bakelite and the copper plug.

Using the graphical solution mentioned previously, and the recorded temperature history of the plug, it can be shown that for the heating time involved in this experiment $q_1 \simeq q_2$ at the start of the plug cooling or test run. This further amplifies the need for taking into account correctly the heat loss to the bakelite if the gas heat transfer coefficient is to be evaluated with reasonable accuracy.

Now note the quantities variable with time in equations (2) and (3). In (2) $(t_\theta - t_{aw})$ decreases with time of cooling; likewise, in (3) $(\partial t/\partial r)_b$ decreases with time of cooling for the test conditions. It is possible to write $(\partial t/\partial r)_b$ as $\frac{t_\theta - t_r}{\Delta r}$ where $(t_\theta - t_r)$ is the variable. This presupposes that the plug, bakelite interface thermal resistance is negligible and $\Delta r << r$.

Then it remains to compare $(t_\theta - t_{aw})$ and $(t_\theta - t_r)$ for the cooling time of the plug. Due to the thermal energy storage in the bakelite, t_r will increase with time whereas t_{aw} will remain constant. Therefore, as the plug cools $(t_\theta - t_r)$ will approach zero more rapidly than $(t_\theta - t_{aw})$ since t_r must of necessity be greater than t_{aw} at the beginning of the cooling time.

Also, since $(t_\theta - t_{aw})$ is not zero when $t_\theta = t_r$, thermal energy will continue to flow from the plug into the gas stream with the result that $(t_\theta - t_r)$ becomes negative. Then it is seen that heat flow rate from the plug during the initial part of the cooling curve is given by the equation $q_T = q_1 + q_2$; whereas during the latter portion it will be $q_T = q_1 - q_2$.

When $t_\theta = t_r$, $q_2 = 0$ and equation (1) is valid. This sugg that if the time θ at which $q_2 = 0$ could be predicted precis and were in a suitable portion of the cooling curve, equatic could be used at this point on the cooling curve to predict

However, it is only possible to predict this point approximately since a graphical solution is the only means of prediction. But q_2 is approximately zero compared to q_1 for a considerable time interval on either side of the point $q_2 \equiv 0$. Specifically, for $q_2 \leq 10\% \; q_1$ $\Delta\theta \geq 10$ sec. for this experimental apparatus. Since the total usable portion of the cooling run is 30 to 60 seconds duration, it is seen that $\Delta\theta \geq 10$ sec. covers a considerable portion of this curve. Also, from graphical prediction this range of interest is in the usable portion of the curve. This is shown in Fig. 8 which is a typical time-temperature cooling curve.

Therefore, by confining the analysis of the time-temperature cooling curve to the region just specified, it is possible to use equation (1) and evaluate the gas stream heat transfer coefficient directly.

Before this can be done it is necessary to predict in what portion of the curve $q_2 \leq 10\% \; q_1$. This will depend on the following variables:

(a) Plug heating time
(b) Maximum temperature of the plug above
(c) Gas film heat transfer coefficient
(d) Ratio of area of plug exposed to gas stream and bakelite

By appropriate experimental technique (a), (b), (d) can be held constant for all tests and plugs. Therefore the location on the cooling curve of $q_2 \leq 10\% \; q_1$ will be dependent only on h_1. From a series of graphical predictions for various values of h_1 in the range of interest, the location on the cooling curve of $q_2 \simeq 0$ was determined. It was found that for the range of h_1 of concern the point of $q_2 \simeq 0$ was approximately a fixed portion of the total temperature rise of the plug above t_{aw}.

This basis of interpreting the data was then used to evaluate h_1 along with physical observation of the time-temperature cooling curve to see which group of points, in the region $q_2 \simeq 0$, would yield the best straight line.

Fig. (11) shows the graphical solution for the predicted time-temperature history during the heating of a plug.

Fig. (12) is the graphical solution for the cooling time temperature history. Note the point of $q_2 = 0$ is at approximately $t_\theta / t_{\theta_{max}} = .15$.

As a further check on the validity of the graphical solution, thermocouples were buried in the bakelite at specified radial distances from one of the test plugs. Thus time-temperature

histories of these radial points were also obtained. Superimposed on these results were the results predicted by the graphical solution. The comparison is made in Fig. (13).

The thermocouples were buried near the gas stream face of the bakelite to determine whether or not the heat flow from the plug into the bakelite was essentially radial. It is to be observed that the graphically predicted time-temperature history compares favorably with the measured results for the thermocouple located 1/16 inch from the test plug. Whereas, the measured results are appreciably lower than the predicted for the thermocouple 1/8 inch from the plug. This is no doubt due to the heat loss from the bakelite to the gas stream.

From these results it may be concluded that the heat flow from the plug to the bakelite is essentially radial near the plug and that the graphical solution is satisfactory for these test conditions.

Figure 11 Copper plug temperature rise versus radial distance on a log scale with time as a parameter.

Graphical solution of time-temperature history of bakelite surrounding a copper plug while the plug is being heated.

Figure 12 Copper plug temperature decline versus radial distance on a log scale with time as a parameter.

Graphical solution of time-temperature history of bakelite surrounding a copper plug while the plug is being cooled by the high velocity gas stream.

Figure 13 Temperature above adiabatic wall versus time.

Comparison of graphically predicted, and experimentally measured temperature-time histories for two points in bakelite surrounding a copper plug.

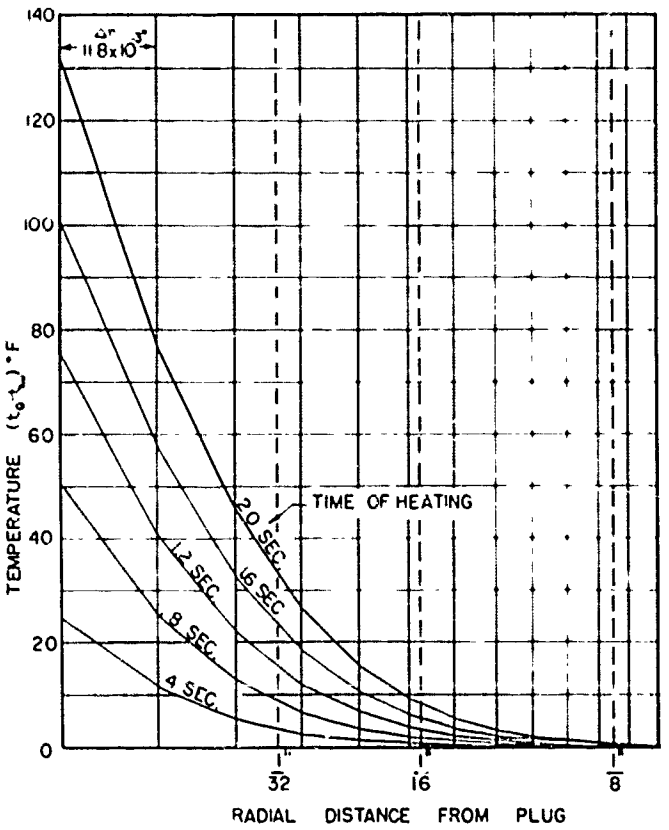

FIGURE 11

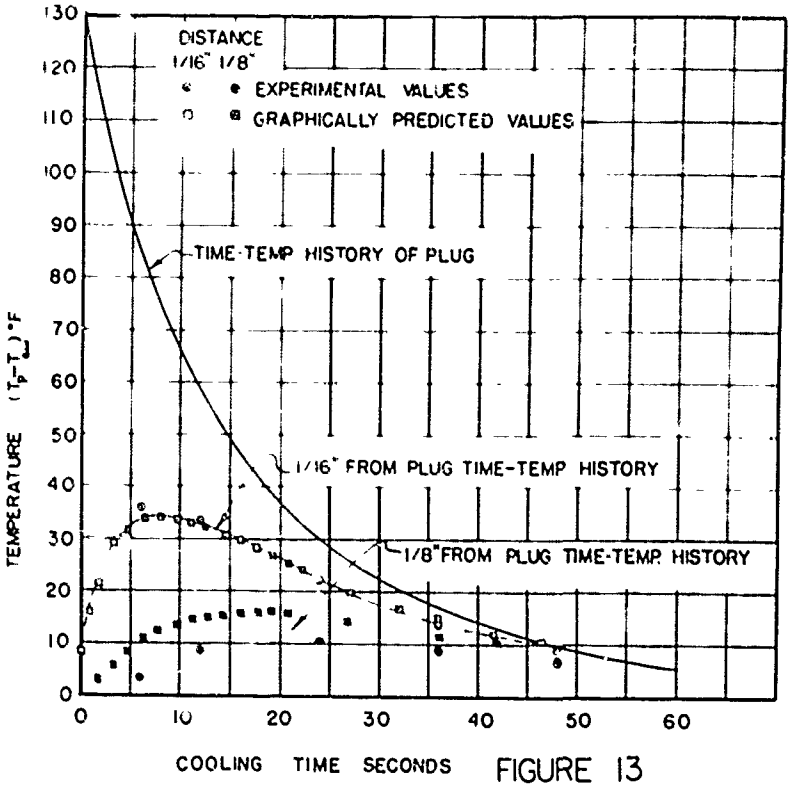

FIGURE 13

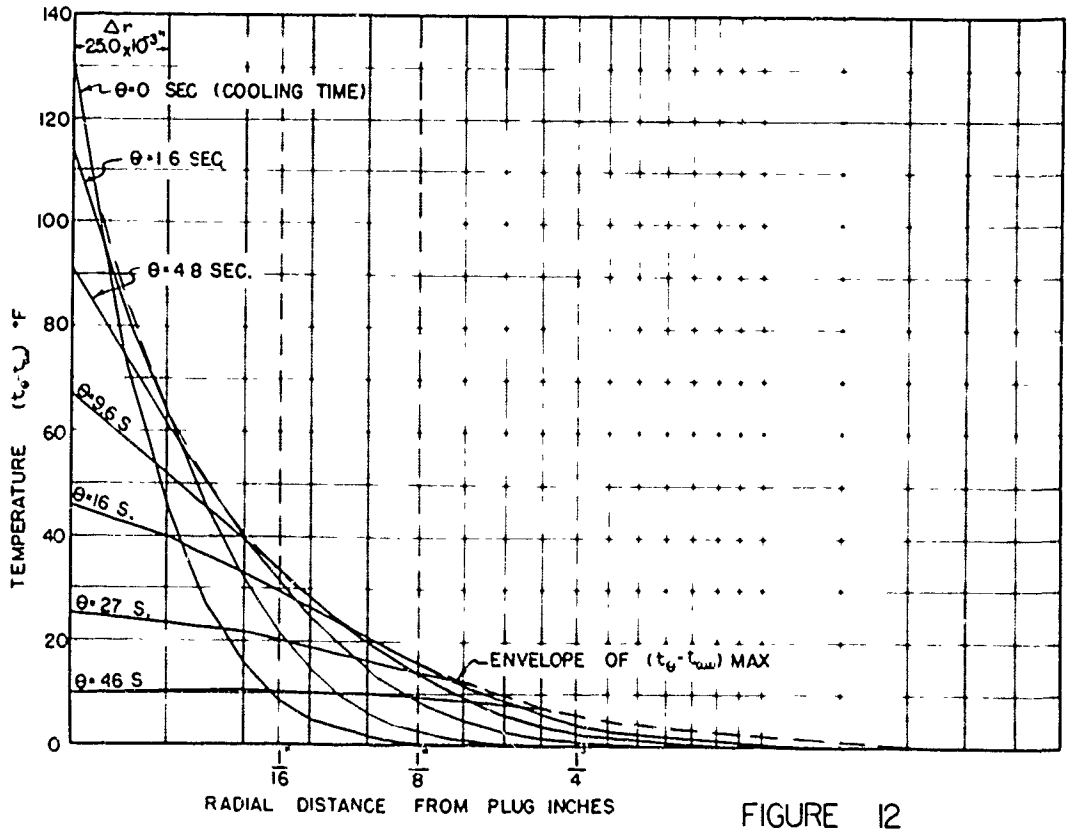

FIGURE 12

ABSTRACT

The objectives of this program are to determine the local convection heat transfer coefficients in the convergent portion and throat sections of de Laval nozzles; and to determine the effect on the local heat transfer coefficients, particularly at the throat, of varying the contour in the converging section of the nozzle.

Three two-dimensional nozzles (described hereafter as III, IV, V), with pressure gradients as defined in Fig. 1a, and resulting cross-sectional areas as described in Fig. 1b, have been tested. Heat transfer coefficients have been obtained for both the flat and contoured walls.

The results do not correlate when using a length dimension based on hydraulic diameter, as conventionally employed for established pipe flow.

The results, for both the flat and contoured walls, do correlate, when using a length dimension measured from the nozzle entrance along the walls. However, the heat transfer coefficients are higher than for turbulent boundary layer flat-plate flow. This appears to be partially due to the technique used in obtaining the apparently local coefficients, and partially due to the negative pressure gradient effect.

A significant result of these tests is that the throat coefficients, for the same mass flow rates through all the nozzles III, IV, and V, agree within ± 15%, indicating that the markedly different throat approach contour variations shown in Fig. 2 do not produce significant variations in the nozzle throat coefficients.

A theoretical solution, predicting the local heat transfer coefficients along the flat wall of nozzle III, has been made by introducing the pressure gradient of nozzle III into the von Karman boundary layer momentum equation. The results of this work are compared to the experimental findings, and are utilized to interpret the experimental results.

PREDICTION OF THE TIME-TEMPERATURE HISTORY OF THE THERMAL PLUG, WHILE COOLING, USING A GRAPHICAL TECHNIQUE

In the process of attempting to analyze the time-temperature history of the thermal plug correctly, an approximate method was derived for evaluating the time-temperature history of a body which losses thermal energy via two paths such as the plugs in this experiment.

The method will be described by using the plugs as a basis of analysis but it can readily be seen that the method is adaptable to any similar system.

By making the following assumptions, the cooling time-temperature history of a plug can be predicted as a function of plug dimensions and the gas film heat transfer coefficient.

(a) Assume time of heating plug and temperature to which it is raised are known. Then the temperature distribution in the bakelite at time zero of the cooling run is known.

(b) Assume radial heat flow only from the plug into the bakelite.

(c) Assume the thermal diffusivity of copper with respect to heat flow from its face to the gas stream and from its side area to the bakelite is sufficiently high to consider the plug at isothermal conditions. (This has been verified for the case of the experimental data.)

(d) Assume the contact resistance between the copper and bakelite is negligible.

(e) Assume heat flows from the plug only via the two paths just mentioned.

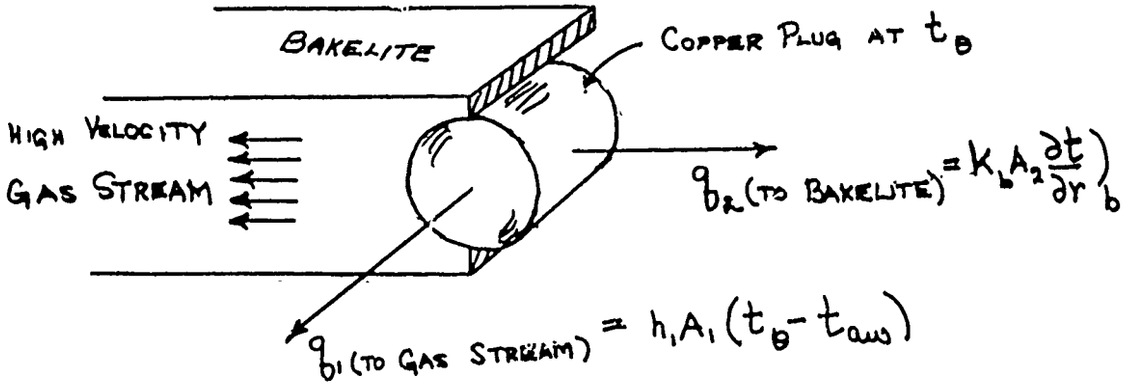

Now $\left(\frac{\partial t}{\partial r}\right)_b$ can be written as $\frac{t_\theta - t_r}{\Delta r}$ if Δr is small as compared to r which is the case here.

First consider the time-temperature cooling history of the plug when the stream face is insulated, $q_1 = 0$.

Then from a consideration of rate equation and energy balance on the plug for a very short time in finite differential form

$$V\rho C\ \Delta t_\theta = \frac{k_b A_2}{\Delta r}\ (t_\theta - t_r)\Delta\theta$$

$$\frac{V\rho C}{k_b A_2}\ \frac{\Delta r}{\Delta \theta} = \frac{t_\theta - t_r}{\Delta t_\theta} \quad - - \qquad (1)$$

Consider the graphical solution described earlier, of the time-temperature history of the bakelite while the plug is heating. It is solved for the plug heating time and a sample solution appears in Fig. (11). If some value Δa is chosen such that $\frac{\Delta t_\theta}{\Delta a} = \frac{t_\theta - t_r}{\Delta r}$ then equation (2) results.

$$\frac{t_\theta - t_r}{\Delta t_\theta} = \frac{\Delta r}{\Delta a} \quad - - - \qquad (2)$$

Substituting equation (2) in equation (1)

$$\frac{V\rho C}{k_b A_2} \cdot \frac{\Delta r}{\Delta \theta} = \frac{\Delta r}{\Delta a}$$

$$\Delta a = \frac{k_b A_2 \Delta \theta}{V\rho C}$$

This is assuming $(t_\theta - t_r)$ is constant for time $\Delta\theta$. Actually, if Δa is small compared to Δr this is very nearly true.

Since all the physical properties other than temperature are previously related or known in order to make the graphical solution of the time-temperature history of the bakelite while the plug is heating; it remains to introduce Δa into the graphical solution to predict the time-temperature history of the plug during the cooling run. By laying it out as shown in the following figure t_θ' which equals $t_\theta - \Delta t_\theta$ can be laid off directly and the time-temperature history of the plug and bakelite matrix can be predicted in rapid fashion.

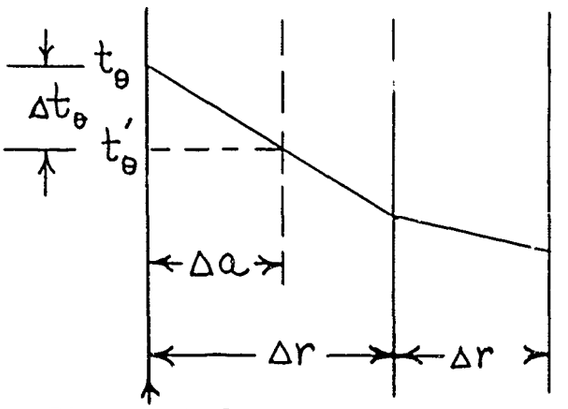

In the case where there is heat loss to the bakelite and gas stream simultaneously, divide the mass of the plug into two components $V\rho)_1$ and $V\rho)_2$. Let one supply thermal energy to the gas stream and one supply thermal energy to the bakelite.

Then from consideration of thermal energy flow rates and energy balance on the plug the following two equations are obtained:

$$V\rho)_1 C \frac{\Delta t_\theta}{\Delta \theta} = h_1 A_1 (t_\theta - t_{aw}) \quad (4)$$

$$V\rho)_2 C \frac{\Delta t_\theta}{\Delta \theta} = k_b A_2 \left(\frac{t_\theta - t_r}{\Delta r}\right) \quad (5)$$

The $\Delta\theta$ to be used is evaluated from the physical properties and the selected value of Δr for the graphical solution.

Δt_θ must be the same in equations (4) and (5). Then solving for $\frac{\Delta t_\theta}{\Delta \theta}$ in both equations and equating gives

$$\frac{h_1 A_1}{V\rho)_1}(t_\theta - t_{aw}) = \frac{k_b A_2}{V\rho)_2}\ \frac{(t_\theta - t_r)}{\Delta r} \quad -- \tag{6}$$

$$\text{or} \quad \frac{t_\theta - t_{aw}}{t_\theta - t_r} = \frac{V_1}{V_2}\ \frac{k_b A_2}{h_1 A_1 \Delta r} \quad -- \tag{7}$$

Let $\frac{k_b A_2}{h_1 A_1 \Delta r} = \gamma$ which is a constant for any cooling run.

Then equation (7) becomes

$$\frac{t_\theta - t_{aw}}{t_\theta - t_r} = \left(\frac{V}{V_2} - 1\right)\gamma \qquad \text{where } V = V_1 + V_2$$

$$\text{or} \quad V_2 = \frac{V}{1 + \frac{1}{\gamma}\ \left(\frac{t_\theta - t_{aw}}{t_\theta - t_r}\right)} \quad -- \tag{7a}$$

Substituting equation (5) in equation (7) gives:

$$\frac{\Delta t_\theta}{t_\theta - t_r} = \frac{k_b A_2 \Delta\theta}{V\rho)_2 C \Delta r} = \frac{k_b A_2 \Delta\theta}{\rho C V \Delta r}\left[1 + \frac{1}{\gamma}\ \frac{(t_\theta - t_{aw})}{(t_\theta - t_r)}\right] -- \tag{8}$$

Letting $\frac{\Delta t_\theta}{\Delta a} = \frac{t_\theta - t_r}{\Delta r}$

or $$\frac{\Delta t_\theta}{t_\theta - t_r} = \frac{\Delta a}{\Delta r} \quad -- \quad (9)$$

Substituting equation (9) in equation (8) gives

$$\frac{\Delta a}{\Delta r} = \frac{k_b A_2 \Delta \theta}{V \rho C \Delta r} \left[1 + \frac{1}{\gamma} \frac{(t_\theta - t_{aw})}{(t_\theta - t_r)}\right] \quad -- \quad (10)$$

Letting $$\frac{k_b A_2 \Delta \theta}{V \rho C \Delta r} = \beta = \text{Constant}$$

$$\frac{\Delta a}{\Delta r} = \beta \left[1 + \frac{1}{\gamma} \frac{(t_\theta - t_{aw})}{(t_\theta - t_r)}\right] \quad -- \quad (11)$$

Now β, γ, t_{aw}, Δr are all constants. $(t_\theta - t_r)$ and $(t_\theta - t_{aw})$ can be read from the graphical solution.

To predict time-temperature cooling history of a plug then the procedure would be exactly the same as in the case where the gas stream face of the plug was insulated except that in this case $\frac{\Delta a}{\Delta r}$ is not constant but will have to be evaluated each time as a function of $\frac{t_\theta - t_{aw}}{t_\theta - t_r}$.

It is seen that $\frac{\Delta a}{\Delta r}$ will vary as a function of $\frac{t_\theta - t_{aw}}{t_\theta - t_r}$. In this case $(t_\theta - t_{aw})$ will decrease less rapidly than $(t_\theta - t_r)$. Therefore $\frac{\Delta a}{\Delta r}$ will approach a very large quantity and the solution will be invalid in this region. However, as $(t_\theta - t_r)$ approaches zero the heat

loss to the bakelite becomes negligible and Δt_θ can be evaluated in this region by

$$\frac{\Delta t_\theta}{\Delta \theta} = \frac{h_1 A_1}{V \rho C} (t_\theta - t_{aw})$$

This method was used to repredict the cooling time-temperature history using the heat transfer coefficient determined by the method described earlier in the appendix.

The results are shown in Fig. (14). The repredicted time-temperature history shows very good comparison with the measured time-temperature history of the plug and it is concluded from these results that both the method just described and the method of determining the heat transfer coefficient are valid.

Figure 14 Temperature of copper plug above adiabatic wall temperature versus time.

Comparison of the experimentally measured time-temperature history of the plug and the time-temperature history predicted by a graphical technique.

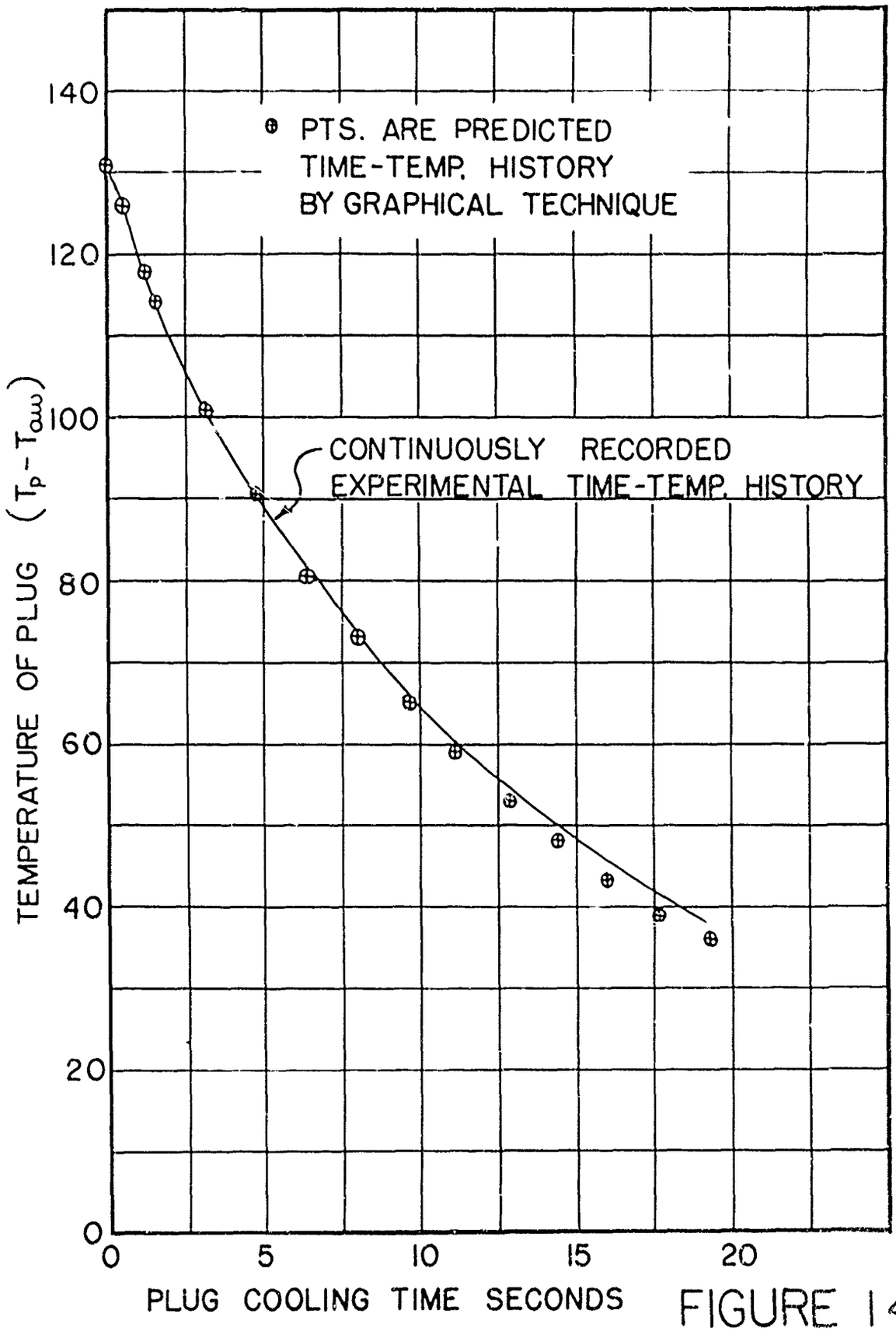
⊕ PTS. ARE PREDICTED
TIME-TEMP. HISTORY
BY GRAPHICAL TECHNIQUE
CONTINUOUSLY RECORDED
EXPERIMENTAL TIME-TEMP. HISTORY
TEMPERATURE OF PLUG ($T_p - T_{aw}$)
PLUG COOLING TIME SECONDS
0
20
40
60
80
100
120
140
0
5
10
15
20

FIGURE 14

INVESTIGATION OF THE THERMAL PLUG EFFECT IN ESTABLISHED, TURBULENT PIPE FLOW

To obtain more quantitative experimental evidence of the significance of the delayed thermal boundary layer with respect to the hydrodynamic boundary layer a plug identical in geometry to those used in the nozzle experiments was placed in the wall of a pipe, insulated from the pipe by a bakelite annulus, and both the bakelite and plug were machined flush with the inner surface of the pipe. The same transient technique was used to obtain the heat transfer coefficient in this test apparatus as was used in the nozzle experiments.

The flow rate was sufficiently high, $Re_D = 2.44 \times 10^5$, and the pipe length great enough, L/D of 70, to assure established turbulent pipe flow.

The predicted Stanton No. based on the correlation

$$St\ Pr^{2/3} = .023\ Re_D^{-.2}$$

was St. No. = 2.46×10^{-3} .

The experimental St. No. value obtained using the thermal plug was

$$St.\ No. = 5.70 \times 10^{-3} \quad .$$

If Stanton's No. were predicted on a flat plate basis using the maximum velocity of the pipe as the free stream velocity for flow over a flat plate and the length in the Reynolds No. as 1/2 the length of a square plug equivalent in area to the round plug tested, the Stanton No. value based on the correlation

$$St\ Pr^{2/3} = .0295\ Re_x^{-.2}$$

would be St. No. = 6.25×10^{-3} .

It was anticipated that the experimental results would lie between the Stanton No. predicted for established flow and established thermal boundary layer and the Stanton No. predicted on a flat plate basis considering both the thermal and hydrodynamic boundary layers as starting at the leading edge of the thermal plug.

The conclusions that can be drawn from the experimental results are:

1) The anticipation of the results lying between the two limits just described is valid.

2) That the results are nearer the upper limit $St = 6.25 \times 10^{-3}$.

STANFORD UNIVERSITY
Technical Reports Distribution List
Contract N6-onr-251 Task Order 6

Chief of Naval Research
Navy Department
Washington 25, D. C.
Attn: Code 438 2
Code 429 1

Director, Naval Research Laboratory
Washington 25, D. C.
Attn: Technical Information Officer 9
Code 500, Mech. Division 1

Commanding Officer
Office of Naval Research
Branch Office
801 Donahue Street
San Francisco 24, California 2

Office of the Assistant Naval Attache for Research
Naval Attache
American Embassy
Navy #100
Fleet Post Office
New York, New York 2

Commanding Officer
Office of Naval Research
Branch Office
1030 E. Green Street
Pasadena 1, California 1

Commanding Officer
Office of Naval Research
Branch Office
495 Summer Street
Boston 10, Massachusetts 1

Commanding Officer
Office of Naval Research
Branch Office
America Fore Building
844 North Rush Street
Chicago, Illinois 1

Commanding Officer
Office of Naval Research
Branch Office
50 Church Street
New York 7, New York 1

Contract Administrator
Southeastern Area
c/o Office of Naval Research
Washington 25, D. C. 1

Bureau of Aeronautics
Navy Department
Washington 25, D. C.
Attn: TD-41, Tech. Library 1
PP-22
(Lt. Cdr. Hoffman) 2

Bureau of Ships
Navy Department
Washington 25, D. C.
Attn: Code 332 2
Code 432 2
Code 641 2
Code 646 10
Code 390 1
Code 434 1
Code 503 1
Code 551 1
Director of Research 5

Superintendent
Post Graduate School
U. S. Naval Academy
Annapolis, Maryland 1

Director,
Naval Engineering
Experiment Station
Annapolis, Maryland
Attn: Capt. W.D. Ligget,Jr. 3
Dr. Senner
(Gas Turbines) 3

Chief of Staff
Dept. of the Army
The Pentagon
Washington 25, D. C.
Attn: Director, Research and Development 1

Commanding General
Air Materiel Command
Wright-Patterson Air Force Base
Dayton, Ohio
Attn: J. B. Johnson, Chief Materials Laboratory 3

Commanding General
U. S. Air Forces
The Pentagon
Washington 25, D. C.
Attn: Research and Development 1

U. S. Atomic Energy Commission
Division of Research
Washington, D. C. 1

U. S. Coast Guard
1300 E Street, N. W.
Washington, D. C.
Attn: Chief, Testing and Development Division 1

National Advisory Committee for Aeronautics
Cleveland Municipal Airport
Cleveland, Ohio
Attn: J. H. Collins, Jr. 2

U. S. Maritime Commission
Technical Bureau
Washington, D. C.
Attn: Mr. Wanless 1

Dean L. M. K. Boelter
School of Engineering
University of California
Los Angeles, California 1

Professor W. H. McAdams
Dept. of Chemical Engineering
Massachusetts Institute of Tech.
Cambridge 39, Massachusetts 1

Professor W. H. Rohsenow
Dept. of Mechanical Engineering
Massachusetts Institute of Technology
Cambridge 39, Massachusetts 1

Stalker Development Company
409 First Street
Bay City, Michigan
Attn: Mr. E. A. Stalker, President 1

Mr. C. C. Ross
Aerojet Engineering Corp.
Azusa, California 3

Mr. S. K. Anderson
Airesearch Company
9851-9951 Sepulveda Blvd.
Los Angeles 45, California 1

Mr. R. Hosmer Norris
General Electric Company
1 River Road
Schenectady 5, New York 1

Mr. H. A. Johnson
Mechanical Engineering
College of Engineering
University of California
Berkeley 4, California 1

Manager of Engineering
Westinghouse Atomic Power Div.
P.O. Box 1468
Pittsburgh 30, Pennsylvania 1

Mr. Dennison, Head of
Research and Development
Elliott Company
Jeanette, Pennsylvania 1

Mr. R. B. Smith
The W. M. Kellogg Co.
Jersey City, New Jersey 1

Professor A. P. Colburn
Chairman,
Division of Chemical
Engineering
University of Delaware
Newark, Delaware 1

Mr. A. Amorosi
Argonne National Laboratory
P. O. Box 5207
Chicago 80, Illinois 1

Professor R. A. Seban
Dept. of Mechanical Engineering
University of California
Berkley, California 1

Professor B. H. Sage
Department of Chemical
Engineering
California Institute of
Technology
Pasadena, California 1

Professor O. A. Saunders
Imperial College of
Science and Technology
London, S. W. 7
England 1

Mr. Carl Wanzinger
Sverdrup and Parcel
Consulting Trust Building
St. Louis, Missouri 1

John Godfrey
Harrison Radiator Division of
General Motors Corp.
Lockport, New York 1

Commander Hoffman
BAR
Lockheed Aircraft Company
Burbank, California 1

Mr. Fixman
Engineering Design
San Francisco Naval Shipyard
Hunters Point
San Francisco, California 1

Code 300, Building 101
San Francisco Naval Shipyard
Hunters Point
San Francisco, California 1

Mr. V. J. Skoglund
4939 Canterbury Drive
San Diego 4, California 1

E. J. LeFevre
Mechanical Engineering
Research Organization
Dept. of Scientific and
Industrial Research
Rex House
A-12, Regent Street
London, S. W. 1, England 1

Dr. Louis Dunn
Jet Propulsion Laboratory
California Institute of Tech.
Pasadena, California 2

Dr. W. Bolay
Technical Director
Aero Physics Laboratory
North American Aviation Corp.
Downey, California 2

Mr. M. Edmund Ellion
Northrop Aircraft, Inc.
Hawthorne, California 2

Mr. Tom Carvey
6647 West 84th Street
Los Angeles, California 1

Douglas Aircraft Co., Inc.
Technical Library
Santa Monica, California 2

Colonel Homer A. Boushey
Directorate of Research and
Development Office
DCS/Development
Department of the Air Force
Headquarters United States
Air Force
Washington 25, D. C. 1

Project Squid
Princeton University
Princeton, New Jersey
Attn: Miss Jean Newman 1

Dr. M. Tribus
University of Michigan
Ann Arbor, Michigan 1

Commander W. W. Brown
Mare Island Naval Shipyard
Vallejo, California 1

Professor F. L. Schwartz
University of Michigan
Ann Arbor, Michigan 1

Capt. W. A. Dolan
Bureau of Ships
Navy Department
Washington 25, D. C. 1

Dr. J. T. Tettaliata
Director, Dept. of Mech. Eng.
Illinois Institute of Technology
3300 Federal Street
Chicago 16, Illinois 1

Mr. S. A. Tucker
Standards Manager, The
American Society of Mech. Eng.
29 West 39th Street
New York 18, N. Y. 1

Prof. E. M. Fernald
Lafayette College
Eaton, Pennsylvania 1

Mr. H. B. Nottage
American Society of Heating
and Ventilating Engineers
7218 Euclid Avenue
Cleveland 3, Ohio 1

Mr. W. V. Hurley
Aircraft Gas Turbine
Engineering Division
General Electric Company
West Lynn, Mass. 1

Mr. L. J. Fischer
Aircraft Gas Turbine
Engineering Division
General Electric Company
West Lynn, Mass. 1

Mr. Robert C. Sale
Chief Librarian, Research
Department
United Aircraft Corp.
East Hartford, Connecticut 1

Dr. Stewart Way
Westinghouse Research
Laboratory
East Pittsburgh, Pa. 1

Prof. W. J. King
Dept. of Engineering
University of California
Los Angeles, Calif. 1

Mr. L. N. Rowley
McGraw-Hill Publishing Co.
330 W. 42nd Street
New York 18, N. Y. 1

Mr. Gardner L. Locke
General Electric Company
Nucleonics Department
Hanford Works
Richland, Washington 1

Mr. M. Sulkin
Thermodynamics Group
North American Aviation Corp.
Los Angeles Airport
Los Angeles, Calif. 1

Mr. E. A. Ryder
Consulting Engineer
Pratt and Whitney Aircraft
Hartford, Connecticut 1

Mr. Neil Lansing
Oak Ridge National Laboratory
Oak Ridge, Tenn. 1

Mr. E. B. Delson
ANP Project
P. O. Box 125
Oak Ridge, Tenn. 1

Dr. H. F. Poppendiek
Oak Ridge National
Laboratory
P. O. Box P
Oak Ridge, Tenn. 1

Mr. Ned C. Rice, Jr.
Research Department,
United Aircraft Corp.
East Hartford 8, Conn. 1

Mechanical Engineering Dept.
Stanford University 2

Dean Terman
School of Engineering
Stanford University 1

Additional copies for Project
Leader and assistants, Office
of Research Coordination, and
reserve for future requirements 16

Engineering Library
Stanford University 2

Dr. Chauncey Starr
Technical Director
Atomic Energy Research Dept.
North American Aviation
Downey, Calif. 1

Mr. H. S. Mickley
Dept. of Chemical Engineering
Mass. Inst. of Technology
Cambridge 39, Mass. 1

Dr. R. A. Lyon
Oak Ridge National
Laboratory
P. O. Box P
Oak Ridge, Tenn. 1

Mr. Stephen Kline
Department of Mech. Eng.
Mass. Inst. of Technology
Cambridge 39, Mass. 1